

1
2
3
4
5
6
7
8
9
10
11
12
13
14
15
16
17
18
19
20
21
22
23
24
25
26
27
28
29
30
31
32
33
34
35
36
37
38
39
40

Sustained VEGF Delivery Via PLGA Nanoparticles Promotes Vascular Growth

Justin S. Golub¹, Young-tae Kim⁴, Craig L. Duvall^{1,4},
Ravi V. Bellamkonda^{1,4}, Divya Gupta², Angela S. Lin^{1,3}, Daiana Weiss², W. Robert Taylor^{1,2,4},
Robert E. Guldberg^{1,3}

¹ Institute for Bioengineering and Bioscience, Georgia Institute of Technology, Atlanta, Georgia

² Department of Medicine, Division of Cardiology, Emory University School of Medicine and the Atlanta VA Medical Center, Atlanta GA

³ George W. Woodruff School of Mechanical Engineering, Georgia Institute of Technology, Atlanta, Georgia

⁴ Wallace H. Coulter Department of Biomedical Engineering, Georgia Institute of Technology and Emory University, Atlanta, Georgia

Running Title: Sustained VEGF Delivery Via PLGA Nanoparticles

Correspondence:

Robert E. Guldberg, PhD
315 Ferst Drive
Institute for Bioengineering and Bioscience
Georgia Institute of Technology
Atlanta, GA 30332
Phone: 404-894-6589
Fax: 404-385-1397
E-mail: robert.guldberg@me.gatech.edu

41 Abstract

42

43 Technologies to increase tissue vascularity are critically important to the fields of tissue
44 engineering and cardiovascular medicine. Currently, limited technologies exist to encourage
45 angiogenesis and arteriogenesis in a controlled manner. We describe here an injectable
46 controlled release system consisting of vascular endothelial growth factor (VEGF) encapsulated
47 in poly(lactic-*co*-glycolic acid) (PLGA) nanoparticles (NP). The majority of VEGF was released
48 gradually over 2-4 days from the NPs as determined by an ELISA release kinetics study. An *in*
49 *vitro* aortic ring bioassay was used to verify the bioactivity of VEGF-NP compared to empty NP
50 and no treatment. A mouse femoral artery ischemia model was then used to measure
51 revascularization in VEGF-NP treated limbs compared to limbs treated with naked VEGF and
52 saline. 129/Sv mice were anesthetized with isoflurane and a region of the common femoral artery
53 and vein was ligated and excised. Mice were then injected with VEGF-NP, naked VEGF, or
54 saline. After four days, 3D microcomputed tomography (microCT) angiography was employed
55 to quantify vessel growth and morphology. Mice receiving VEGF-NP treatment showed a
56 significant increase in total vessel volume and vessel connectivity compared to 5 µg VEGF, 2.5
57 µg VEGF, and saline treatment (all $p < 0.001$). When taking the yield of the fabrication process
58 into account, VEGF-NPs were over an order of magnitude more potent than naked VEGF in
59 increasing blood vessel volume. Differences between VEGF-NP and all other groups were even
60 greater when analyzing only small-sized vessels under 300 µm diameter. In conclusion,
61 sustained VEGF delivery via PLGA nanoparticles shows promise for encouraging blood vessel
62 growth in tissue engineering and cardiovascular medicine applications.

63

64 **Keywords:** tissue engineering, nanoparticle, angiogenesis, arteriogenesis, VEGF

65

66 **Introduction**

67

68 Technologies to enhance angiogenesis and arteriogenesis are greatly needed in
69 cardiovascular medicine and tissue engineering. Limited options currently exist to increase tissue
70 vascularity in a controlled manner. The most widely-employed vasculogenic agent, vascular
71 endothelial growth factor (VEGF) has been previously shown to enhance revascularization *in*
72 *vivo*(8, 16, 17). However, human clinical trials have been disappointing because therapeutic
73 effects are achieved only at extremely high doses. This often results in side effects such as
74 hypotension, retinopathy, or progression of malignant tumors.(5, 6).

75 A controlled released system could increase treatment efficacy, thus allowing for a lower
76 dose of growth factor. With the extraordinary expense associated with growth factor therapy, the
77 economic advantages are also attractive. Moreover, sustained release of VEGF may be necessary
78 for the maintenance of stable neovessels.(11) An injectable system is additionally appealing
79 because it obviates the need for surgical implantation of drug delivery devices, such as scaffolds
80 or osmotic minipumps. An injectable controlled release strategy thus allows for minimally
81 invasive delivery with convenient and infrequent dosing.

82 Poly(lactic-*co*-glycolic acid) (PLGA) copolymer is an attractive delivery vehicle because
83 of its excellent biocompatibility, high safety profile, widespread use in medicine, and FDA-
84 approval for usage in drug delivery.(7, 9) Injectable PLGA delivery systems involve
85 encapsulation of a growth factor. As the PLGA capsule is hydrolytically degraded over time *in*
86 *vivo* or *in vitro*, growth factor is released into the surrounding region. This method confers a
87 notable advantage over sustained release via gene therapy, which has mutagenic and tumorigenic
88 potential. In addition, the release kinetics of this system can be easily adjusted by altering the

89 ratio of PLA:PGA. Recently, focus has shifted to encapsulation of bioactive substances with
90 particles of a nanometer scale. Nanoparticle encapsulation confers several advantages over
91 microparticle encapsulation, including a lower risk of embolization(2, 13).

92 In this study, a mouse femoral artery ligation model of hind limb ischemia was used to
93 evaluate the efficacy of VEGF-NP in inducing vascular growth. Analysis included the use of 3D
94 microcomputed tomography (microCT) angiography, which, to our knowledge has never been
95 employed before to analyze vascular formation stimulated by sustained delivery of VEGF.

96

97 **Materials and Methods**

98

99 *VEGF-NP Fabrication*

100 VEGF encapsulated PLGA nanoparticles (VEGF-NP) were fabricated by modification of
101 the double emulsion (water/oil/water phase) method.(7) Briefly 100 mg 2% (w/v) 50:50 PLGA
102 copolymer (Polysciences, Warrington, PA) was dissolved in 5 mL of dichloromethane (DCM).
103 Recombinant murine VEGF (Chemicon/Millipore; Billerica, MA) was dissolved in 250 μ L of
104 sterilized 0.2% BSA in deionized water. VEGF solution was then added to the pre-ice cooled
105 PLGA solution. Emulsification of VEGF in PLGA was then performed by homogenization at
106 4000 rpm at 13 sec/run for three runs. This emulsion was added to poly(vinyl alcohol) (PVA)
107 solution (0.4% w/v in sterilized deionized water) and homogenized at 7000 rpm at 18 sec/run for
108 three runs. The double emulsion was diluted in 0.1% PVA solution and DCM was removed by
109 evaporation under reduced pressure for 3 hours. VEGF-NPs in 0.1% PVA solution were
110 collected by centrifugation at 8,500 G for 15 min and washed twice with sterilized deionized
111 water. VEGF-NPs were subsequently lyophilized and stored at -20°C in a desiccator. All steps
112 were conducted under sterile conditions. For size characterization, VEGF-NPs were suspended
113 in 1X PBS and analyzed on a Hitachi H-7500 transmission electron microscope.

114

115 *Release Kinetics*

116 Release kinetics of VEGF-NPs were characterized *in vitro* using an ELISA-based assay.
117 VEGF-NPs were mixed with 0.6% SeaPlaque agarose (Cambrex; East Rutherford, New Jersey)
118 and gelled at 4°C. 1X PBS was then added above the agarose and incubated at 37°C. At days 1,
119 2, 3, 4, 6, 8, 10, 12, 14, and 21 of incubation under standard tissue culture conditions (37° C, 5%

120 CO₂), 1X PBS was collected followed by replacement with fresh PBS. The assay was performed
121 in quadruplicate. Released VEGF concentrations from collected samples were then measured
122 with ELISA (PeproTech; Rocky Hill, NJ). Cumulative VEGF mass release per PLGA NP mass
123 was calculated to determine effective loading yield (i.e. encapsulation efficiency) of VEGF in
124 NPs.

125

126 *In Vitro Bioassay*

127 To determine bioactivity of VEGF and VEGF-NP, a mouse aortic ring assay was
128 performed as previously described.(10) Briefly, 1 mm long aortic rings were harvested from
129 freshly sacrificed 8-10 week old male C57Bl6/J mice (Jackson Laboratory; Bar Harbor, Maine).
130 Explants were embedded in 1.5 mg/mL collagen gels (Serva Chemical) placed inside of agarose
131 wells. In addition to 2.5% murine serum harvested from C57Bl6/J mice, 2.3 mg VEGF-NP, 2.3
132 mg saline encapsulated nanoparticles-NP (Saline-NP), or an equivalent volume of saline was
133 added to 6 mL of molecular, cellular, and developmental biology (MCDB) 131 media. Nine
134 replications were performed. At days 4, 6, 8, and 10, total sprout number and maximum sprout
135 length was recorded using an Olympus inverted microscope.

136

137 *Hind Limb Ischemia Surgery and Injection*

138 All surgeries were performed on 7-8 week old female 129/Sv mice (Charles River
139 Laboratories; Wilmington, MA). Protocols were approved by the Institutional Animal Care and
140 Use Committee (IACUC) of the Georgia Institute of Technology and were performed in
141 accordance with the NIH *Guide for the Care and Use of Laboratory Animals*.

142 The mouse femoral artery ligation model was employed to study collateral vessel

143 formation.(1, 3) Anesthesia was induced with 5% isoflurane in 1000 mL/min oxygen and
144 maintained with 2% isoflurane gas in 350 mL/min oxygen. A 3 cm incision was made over the
145 right medial thigh. The common femoral artery and vein were then ligated at three points: 1)
146 proximal to the superficial epigastric artery, 2) proximal to the bifurcation of the tibial arteries,
147 and 3) at a deep branching radical approximately 1 cm distal to the proximal ligation point. The
148 last ligation was required for hemostasis. The length of artery and vein was then excised between
149 the ligation points. This was followed by six 25 μ L saline or treatment/saline injections with a
150 29G syringe in the ischemic thigh adductor muscles between the ligation points for a total
151 injection volume of 150 μ L per mouse. Depending on the assigned group, each animal received 5
152 μ g VEGF (n=13 for microCT), 2.5 μ g VEGF (n=11 for microCT), 8 mg of VEGF-NP (n=12 for
153 microCT, n=3 for histology), 8 mg of empty-NP (n=5 for microCT), or saline (n=16 for
154 microCT, n=2 for histology). Based on release kinetics data, 8 mg of VEGF-NP delivered 375 ng
155 of VEGF. An additional group of mice (n=7 for microCT) was not injected and was perfused
156 immediately following surgery to establish a baseline. The skin was closed with simple
157 interrupted silk sutures.

158 Buprenorphine (0.03 mg/kg subcutaneous injection one time upon awakening) was
159 provided for analgesia. Mice were allowed to ambulate freely postoperatively. Within 2 days
160 nearly all mice were able to use the operated hind limb. Chewing at sutures was not a noted
161 postoperative behavior. No mice had appreciable postoperative leg swelling, inflammation, or
162 infection. Four days after surgery, animals were sacrificed by ketamine/xylazine overdose and
163 perfused with heparinized saline and 10% neutral buffered formalin as previously described.(3)
164 Mice in the day 0 group were perfused 2 hours after surgery.

165

166 *Microcomputed Tomography*

167 Samples were prepared for microcomputed tomography (microCT) using a previously
168 described procedure.(3) Immediately following standard formalin fixation, mice were perfused
169 with 6 mL of silicone/lead chromate contrast agent (Microfil MV-122, Flow Tech; Carver, MA).
170 The silicone was allowed to polymerize overnight at 4°C. Hind limbs were separated from the
171 body at the junction of the internal and external iliac arteries, fixed for 48 hrs in 10% neutral
172 buffered formalin, and treated for 48 hrs with a formic acid-based solution for decalcification of
173 bones (Cal Ex II, Fisher Scientific; Pittsburgh, PA). Samples were stored in formalin until
174 scanning.

175 High resolution 3D images were acquired using a microCT imaging system (vivaCT 40,
176 Scanco Medical; Basseldorf, Switzerland). Hind limbs were scanned using a 30 μm isotropic
177 voxel size. The appropriate threshold and imaging parameters were selected to specifically
178 include only perfused vasculature ($\sigma=1$, support=4, threshold=140). System software was used to
179 calculate blood vessel volume, thickness, density, spacing, connectivity, and anisotropy.(12)
180 Blood vessel volume was defined as the total volume contained within blood vessels. Volume
181 was measured in voxels, where 1 voxel was set to equal 27,000 μm . Connectivity was defined as
182 the maximal number of branches that can be broken within a structure before it is divided into
183 two separate parts.(3) Anisotropy is defined as the degree to which a segmented vascular bed is
184 oriented towards a specific direction. The algorithm for calculating anisotropy and other
185 parameters have been detailed in previous studies.(3) Three-dimensional microCT angiograms
186 with color-labeled vessel diameter were also generated to compare overall morphometric
187 differences of collateral vessels between treatment groups.

188 Vessel volume was expressed as a ratio of the operated limb compared to the unoperated
189 limb. In addition, the day 0 ratio was subtracted from each group so that the 0% baseline
190 represented no new vessel growth. For vessel connectivity, the day 0 connectivity was subtracted
191 from the group so that the 0% baseline represented no improvement in connectivity.

192

193 *Immunohistochemistry*

194 Following saline/formalin perfusion, hind limbs were harvested and fixed for 48 hrs in
195 10% neutral buffered formalin. A portion of the adductor muscles were excised and cut into 10
196 μm frozen sections using a cryostat. A biotinylated lectin primary antibody (Vector Labs;
197 Burlingame, CA) was used with streptavidin Texas Red quantum dots (Invitrogen; Carlsbad, CA)
198 to mark capillary endothelial cells. Hoechst was employed as a nuclear counterstain. Samples
199 were also stained with hematoxylin-eosin. Eight sections were chosen at random for qualitative
200 analysis.

201

202 *Statistical Analysis*

203 Statistical analysis was performed in Minitab 12.23. ANOVA was used to compare
204 differences in means between groups. Differences were considered significant if $p < 0.05$. All
205 means values are shown \pm standard error.

206

207 **Results**

208

209 *Size Characterization, Release Kinetics, and Loading Dose*

210 VEGF-NP were approximately 400 nm in diameter, with most particles falling between
211 200 and 600 nm. VEGF was released from 50:50 PLGA nanoparticles over 2 weeks. Release
212 decreased exponentially from day 0, with the majority occurring over 2 days. By 4 days, 89%
213 was released. (Figure 1) The calculated concentration of VEGF in VEGF-NP was 52.9 ng/mg.
214 Thus the estimated dose of VEGF delivered to a mouse hind limb in an 8 mg VEGF-NP injection
215 over the 4 day experiment was approximately 375 ng. The effective loading yield of VEGF
216 during VEGF-NP fabrication was 5.3%.

217

218 *Bioassay*

219 The mouse aortic ring angiogenesis assay demonstrated a significantly increased sprout
220 number in the presence of VEGF-NP compared to both saline ($p=0.001$) and empty-NP ($p<0.05$)
221 (Figure 2). This was consistent across the nine replicates. By day 8, rings in the presence of
222 VEGF-NP contained 32 ± 3 sprouts compared to 19 ± 4 sprouts in the presence of empty NP
223 ($p<0.05$) and 16 ± 3 sprouts in the presence of saline ($p=0.001$). The rate of formation followed a
224 gradual exponential curve and was greatest for the VEGF-NP group.

225

226 *Microcomputed Tomography of Hind limbs*

227 Results from the microCT analysis appear in Figure 3. Mice receiving VEGF-NP
228 treatment showed a significant increase in total vessel volume compared to mice receiving 5 μg
229 VEGF, 2.5 μg VEGF, and saline treatment (all $p<0.001$). A significant increase was also

230 observed for mice receiving 5 μg VEGF compared to saline; however the difference was less
231 than half that observed with mice receiving VEGF-NP. (Figure 3b) Differences between mice
232 receiving VEGF-NP and all other groups were even greater when analyzing only small-sized
233 vessels under 300 μm diameter. (Figure 3c) The value of 300 μm was chosen because it marks
234 the transition between arterioles and arteries and is the general size limit for collateral vessels. A
235 separate *in vivo* study showed no significant difference in vessel growth between saline and
236 empty NP groups. This result was consistent with the *in vitro* aortic ring assay, which also
237 showed an absence of a baseline effect of the nanoparticle delivery vehicle.

238 VEGF-NP treatment induced a statistically significant increase in connectivity compared
239 to saline treatment ($p < 0.05$), which was nearly three-fold in magnitude. Connectivity is defined
240 as the maximal number of branches that can be broken within a structure before it is divided into
241 two separate parts. After an ischemic insult, vessel connectivity decreases dramatically.(3)
242 Connectivity was restored to nearly the same level as that of non-operated limbs. A significant
243 increase was also observed for mice receiving 5 μg VEGF compared to saline ($p < 0.05$); however
244 this difference was lower than that of mice receiving VEGF-NP. A significant increase was not
245 noted for mice receiving 2.5 μg VEGF ($p = 0.13$). (Figure 3d)

246 VEGF-NP treatment caused a significant decrease in mean vessel diameter compared to
247 both 5 μg VEGF treatment and saline treatment ($p < 0.05$). Vessel diameter distribution showed
248 an increase in small vessels under approximately 400 μm diameter for all groups compared to
249 day 0 perfusion baseline mice. However this increase was notably greatest in VEGF-NP treated
250 mice. No increases in large vessels over 400 μm diameter were observed for any groups
251 compared to the day 0 baseline. (Figure 4)

252 No statistically significant differences were seen between VEGF-NP treatment, 5 μ g
253 VEGF treatment, and saline treatment groups for vessel density or spacing. The degree of
254 anisotropy was also statistically unchanged, indicating that there was no difference in the degree
255 to which vessels were oriented in a specific direction.

256 *Histology of Hind Limbs*

257 Through immunostaining of endothelial cells, VEGF-NP treated hind limbs appeared to
258 have greater vessel numbers qualitatively, than saline treated hind limbs. The morphometric
259 arrangement between vessels in the surrounding musculature was similar between VEGF-NP
260 treated hind limbs, saline treated hind limbs, and non-surgery hind limbs. (Figure 5)

261

262 **Discussion**

263

264 We have demonstrated the feasibility of using VEGF-encapsulated nanoparticles (VEGF-
265 NP) to produce a vigorous revascularization response. VEGF-NP treated limbs showed a
266 significant increase in total vessel volume compared to 5 μg VEGF, 2.5 μg VEGF, and saline
267 treatment. The difference was even more pronounced when analyzing only small-to-medium
268 sized vessels under 300 μm diameter. This latter finding agrees with mean vessel diameter data
269 and the vessel diameter distribution data, which showed the greatest peak in vessels at 120 μm .
270 Nearly all vessels that increased in prevalence after VEGF-NP treatment were markedly larger
271 than capillaries (>10 μm diameter). Thus, VEGF-NP did not produce its effect simply by
272 vasodilation of pre-existing capillaries.

273 In addition, VEGF-NP was also the only treatment method that restored blood vessel
274 connectivity to its pre-surgical value. The increase in connectivity demonstrated that VEGF-NP
275 caused structural changes to the vascular bed, such as increased anastomoses. This effect would
276 not have been observed if VEGF-NP merely vasodilated pre-existing vessels.

277 These *in vivo* data also agree with the *in vitro* aortic ring angiogenesis assay data. Aortic
278 rings placed in the presence of VEGF-NP showed significantly more sprouting than aortic rings
279 placed in the presence of empty NP or saline. A preliminary assay employing aortic rings in the
280 presence of unencapsulated VEGF also showed significant sprouting (data not shown). Thus
281 both the VEGF protein itself as well the fabricated VEGF-NP were biologically active.

282 No significant differences were found between VEGF-NP, 5 μg VEGF, and saline
283 treatment for vessel density or spacing. The increase in vessel volume and thickness in the
284 context of an unchanged density or spacing suggests that the treatments did not result in a

285 significant increase in new vessels. Instead, it appears that existing vessels simply became larger
286 or more interconnected with treatment. This supports previous data that ischemia encourages an
287 arteriogenesis pathway (dilation and remodeling of existing arterioles) as opposed to an
288 angiogenesis pathway (de novo formation of capillaries).(3, 14) Anisotropy was also unchanged,
289 indicating that VEGF-NP treatment did not change the degree to which vessels were oriented in
290 a specific direction.

291 For ease of comparison between groups, this study employed only female mice. Future
292 studies should replicate the effects in mice of both sexes. This would determine if the increased
293 presence of estrogen or lack of male hormones would have any added vasculogenic effect in
294 females or whether the effect would be equivalent in males.

295 One potential concern of NP usage is that the NP themselves may cause an immune
296 response, which, in turn, may help to stimulate revascularization. In addition, any organic
297 solvents used in PLGA NP fabrication remaining associated with the particles might further
298 increase the immune response. Both the aortic ring assay and *in vivo* hind limb ischemia
299 experiments demonstrated that empty-NP had no significant effect on vasculogenesis. These
300 results demonstrate that the nanoparticles themselves were not responsible for the observed
301 arteriogenic effect of the VEGF-NP group.

302 Another concern of NP delivery is the possibility of aggregate formation and
303 embolization. Because of the small size of NPs, aggregates would have to be relatively large to
304 produce embolic phenomena. Such aggregates were not seen in *in vivo* (data not shown).
305 Furthermore, microCT demonstrated an increase in the volume of perfused small vessels,
306 arguing against the occurrence of embolism.

307 A limitation of NP delivery is the low yield during fabrication. The effective VEGF
308 loading yield during VEGF-NP fabrication was only approximately 5%. This value was lower
309 than the yield of 22-70% described for similarly fabricated PLGA NPs.(2, 18, 19) However,
310 these assays for measuring loading yield involved mechanically or chemically dissolving NPs
311 encapsulating fluorescent markers immediately after fabrication. It is possible that some of the
312 loaded VEGF was rendered inactive during fabrication or the 21 days of incubation under
313 physiologic conditions. While steps are taken to maintain the stability of the protein during
314 fabrication, it is still possible that some degradation/denaturation may occur. For example,
315 homogenization may produce excessive heat, despite placement of all solutions on ice.
316 Furthermore, hydrolysis of PLGA during the collection phase could produce acidic monomers
317 and oligomers, resulting in VEGF inactivation.(13, 20) While potentially underestimating
318 encapsulation efficiency, the effective loading yield described here more accurately reflects the
319 amount of active VEGF that would be present *in vivo*. A final limitation of the PLGA delivery
320 vehicle is the acidic byproduct of the hydrolysis reaction, which has been shown to be cytotoxic
321 both *in vivo* and *in vitro*.(15) However, our data showed no evidence of an adverse effect of
322 empty nanoparticles alone.

323 MicroCT angiography was the primary method of analysis in this study because of its
324 superior ability to quantify three-dimensional vessel growth. Correlation to standard methods of
325 quantitation, such as immunohistochemistry, has been previously demonstrated.(3) Furthermore,
326 prior studies have shown that microCT measurements of vessel volume and morphology
327 correspond to functional measures such as blood flow and swim endurance.(4)

328 When taking VEGF dosing into account, VEGF-NPs were over an order of magnitude
329 more potent than unencapsulated VEGF in increasing blood vessel volume *in vivo*. After 4 days

330 of release, a single 8 mg dose of VEGF-NP yielded approximately 470 ng of ELISA-detectable
331 VEGF. This is less than 10% of the VEGF dose of the 5 μ g injection group. Yet a significantly
332 increased vasculogenic response was observed in the VEGF-NP treated mice compared to the 5
333 μ g VEGF group. This finding illustrates the increased efficacy of slow, sustained release of
334 growth factor compared to one-time immediate delivery.

335 Despite the strong positive effect observed, several methodological hurdles remain before
336 VEGF-NP can be used clinically. NP fabrication involves use of organic solvents such as PVA,
337 which may remain associated with the nanoparticle surface(13). In addition, the effective loading
338 yield is fairly low. Future optimization of the fabrication protocol could greatly increase this
339 figure, making the process even more economically advantageous compared to naked protein
340 delivery. Despite these challenges, this study suggests that sustained release delivery strategies
341 may provide greater therapeutic benefit at lower overall doses than bolus delivery of
342 vasculogenic proteins and thus provide a viable alternative delivery strategy for use in human
343 disease.

344

345 **Acknowledgements**

346

347 The authors would like to acknowledge Laura O'Farrell for aid with surgical technique. This
348 study was funded by the Georgia Tech/Emory Center for the Engineering of Living Tissues
349 (GTEC) NSF Grant EEC-9731643 and NIH Grants AR051336, U01 HL080711 and R01
350 HL70531.

351

352 **Disclosures**

353

354 The authors have no financial disclosures.

355

356 **References**

357

- 358 1. **Couffinhal T, Silver M, Zheng LP, Kearney M, Witzenbichler B, and Isner JM.**
359 Mouse model of angiogenesis. *Am J Pathol* 152: 1667-1679, 1998.
- 360 2. **Davda J, and Labhasetwar V.** Characterization of nanoparticle uptake by endothelial
361 cells. *Int J Pharm* 233: 51-59, 2002.
- 362 3. **Duvall CL, Taylor WR, Weiss D, and Guldberg RE.** Quantitative microcomputed
363 tomography analysis of collateral vessel development after ischemic injury. *Am J Physiol Heart*
364 *Circ Physiol* 287: H302-310, 2004.
- 365 4. **Duvall CL, Weiss D, Robinson ST, Alameddine FM, Guldberg RE, and Taylor WR.**
366 The role of osteopontin in recovery from hind limb ischemia. *Arteriosclerosis, thrombosis, and*
367 *vascular biology* 28: 290-295, 2008.
- 368 5. **Freedman SB, and Isner JM.** Therapeutic angiogenesis for coronary artery disease. *Ann*
369 *Intern Med* 136: 54-71, 2002.
- 370 6. **Henry TD, Annex BH, McKendall GR, Azrin MA, Lopez JJ, Giordano FJ, Shah**
371 **PK, Willerson JT, Benza RL, Berman DS, Gibson CM, Bajamonde A, Rundle AC, Fine J,**
372 **and McCluskey ER.** The VIVA trial: Vascular endothelial growth factor in Ischemia for
373 Vascular Angiogenesis. *Circulation* 107: 1359-1365, 2003.
- 374 7. **Jain RA.** The manufacturing techniques of various drug loaded biodegradable
375 poly(lactide-co-glycolide) (PLGA) devices. *Biomaterials* 21: 2475-2490, 2000.
- 376 8. **Kofidis T, Nolte D, Simon AR, Metzakis A, Balsam L, Robbins R, and Haverich A.**
377 Restoration of blood flow and evaluation of corresponding angiogenic events by scanning
378 electron microscopy after a single dose of VEGF in a model of peripheral vascular disease.
379 *Angiogenesis* 5: 87-92, 2002.
- 380 9. **Lewis DH.** Controlled release of bioactive agents from lactide/glycolide polymers. In:
381 *Biodegradable polymers as drug delivery systems*, edited by Chasin M, and Langer R. New
382 York: Marcel Dekker, 1990, p. 1-41.
- 383 10. **Masson VV, Devy L, Grignet-Debrus C, Bernt S, Bajou K, Blacher S, Roland G,**
384 **Chang Y, Fong T, Carmeliet P, Foidart JM, and Noel A.** Mouse Aortic Ring Assay: A New
385 Approach of the Molecular Genetics of Angiogenesis. *Biol Proced Online* 4: 24-31, 2002.
- 386 11. **Nagy JA, Vasile E, Feng D, Sundberg C, Brown LF, Detmar MJ, Lawitts JA,**
387 **Benjamin L, Tan X, Manseau EJ, Dvorak AM, and Dvorak HF.** Vascular permeability
388 factor/vascular endothelial growth factor induces lymphangiogenesis as well as angiogenesis. *J*
389 *Exp Med* 196: 1497-1506, 2002.
- 390 12. **Odgaard A, and Gundersen HJ.** Quantification of connectivity in cancellous bone, with
391 special emphasis on 3-D reconstructions. *Bone* 14: 173-182, 1993.
- 392 13. **Panyam J, and Labhasetwar V.** Biodegradable nanoparticles for drug and gene delivery
393 to cells and tissue. *Adv Drug Deliv Rev* 55: 329-347, 2003.
- 394 14. **Scholz D, Ziegelhoeffer T, Helisch A, Wagner S, Friedrich C, Podzuweit T, and**
395 **Schaper W.** Contribution of arteriogenesis and angiogenesis to postocclusive hindlimb perfusion
396 in mice. *J Mol Cell Cardiol* 34: 775-787, 2002.
- 397 15. **Sung HJ, Meredith C, Johnson C, and Galis ZS.** The effect of scaffold degradation
398 rate on three-dimensional cell growth and angiogenesis. *Biomaterials* 25: 5735-5742, 2004.

- 399 16. **Takeshita S, Pu LQ, Stein LA, Sniderman AD, Bunting S, Ferrara N, Isner JM, and**
400 **Symes JF.** Intramuscular administration of vascular endothelial growth factor induces dose-
401 dependent collateral artery augmentation in a rabbit model of chronic limb ischemia. *Circulation*
402 90: II228-234, 1994.
- 403 17. **Takeshita S, Zheng LP, Brogi E, Kearney M, Pu LQ, Bunting S, Ferrara N, Symes**
404 **JF, and Isner JM.** Therapeutic angiogenesis. A single intraarterial bolus of vascular endothelial
405 growth factor augments revascularization in a rabbit ischemic hind limb model. *J Clin Invest* 93:
406 662-670, 1994.
- 407 18. **Yi F, Wu H, and Jia GL.** Formulation and characterization of poly (D,L-lactide-co-
408 glycolide) nanoparticle containing vascular endothelial growth factor for gene delivery. *J Clin*
409 *Pharm Ther* 31: 43-48, 2006.
- 410 19. **Zambaux MF, Bonneaux F, Gref R, Maincent P, Dellacherie E, Alonso MJ,**
411 **Labrude P, and Vigneron C.** Influence of experimental parameters on the characteristics of
412 poly(lactic acid) nanoparticles prepared by a double emulsion method. *J Control Release* 50: 31-
413 40, 1998.
- 414 20. **Zhu G, Mallery SR, and Schwendeman SP.** Stabilization of proteins encapsulated in
415 injectable poly (lactide- co-glycolide). *Nat Biotechnol* 18: 52-57, 2000.
- 416
- 417
- 418

419 **Figure/Table Legends**

420

421

422 **Figure 1.** (a) Transmission electron micrograph of lyophilized 50:50 PLGA VEGF-nanoparticles
423 (VEGF-NP). Scale bar = 1 μm . (b) Release kinetics of 50:50 PLGA VEGF-NP. By 4 days, 89%
424 was released. Values are mean \pm standard error; n=4.

425

426 **Figure 2.** Aortic ring angiogenesis assay. Top: Representative images of aortic rings in the
427 presence of saline, empty NPs, and VEGF-NPs. Discrete sprouts are indicative of a pro-
428 angiogenic environment. Bottom: Mean number of sprouts/ring over time in the various
429 conditions. Nine replicates were performed. The rate of formation followed a gradual
430 exponential curve and was greatest for the VEGF-NP group. Values are mean \pm standard error;
431 n=9 for all groups. * denotes significance between the VEGF-NP group and either of the two
432 control groups at $p < 0.05$.

433

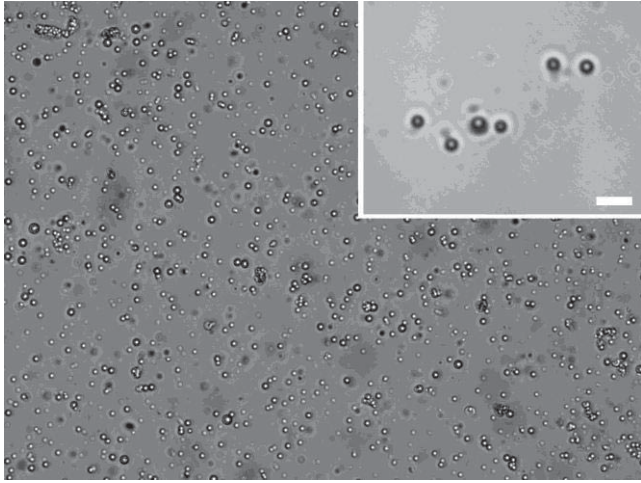
434 **Figure 3.** Limb images and microCT measured parameters. (a) Representative 3D microCT
435 angiograms of treatment groups hind limbs. (b) Surgery limb total vessel volume compared to
436 non-surgery limb. Day 0 vessel volume was subtracted from each group. (c) Surgery limb < 300
437 μm vessel volume compared to non-surgery limb. Day 0 vessel volume was subtracted from each
438 group. (d) Vessel connectivity. Day 0 connectivity was subtracted from each group. For figure
439 parts (b)-(d), n=16 for saline, n=11 for 2.5 μg VEGF, n=13 for 5 μg VEGF, n=12 for VEGF-NP,
440 n=69 for non surgery. Values are mean \pm standard error. ★ denotes significance to all other
441 groups at $p < 0.05$. * denotes significance between two groups at bracket ends at $p < 0.05$.

442

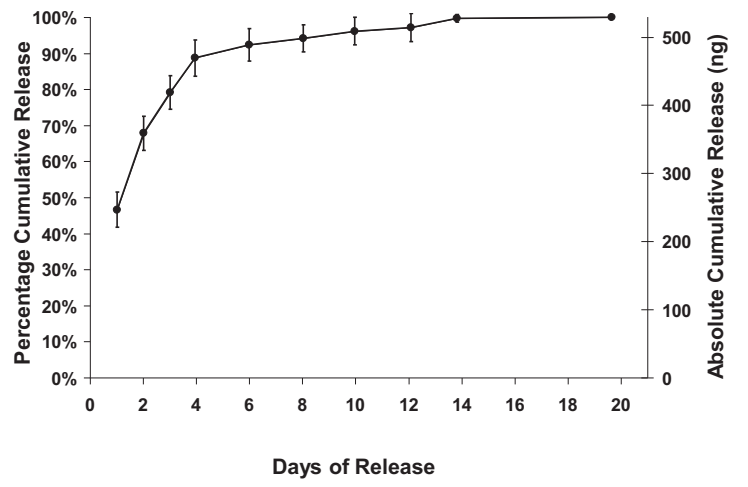
443 **Figure 4.** (a) Distribution of mean vessel diameter of VEGF-NP compared to other experimental
444 and control groups. The X-axis represents vessel diameter and the Y-axis represents the
445 frequency a vessel diameter in encountered. (b) Mean vessel diameter for each experimental and
446 control group. n=16 for saline, n=11 for 2.5 μ g VEGF, n=13 for 5 μ mg VEGF, n=12 for VEGF-
447 NP, n=7 for d0. Values are mean \pm standard error. \star denotes significance to all other groups at
448 $p < 0.05$. * denotes significance between two groups at bracket ends at $p < 0.05$.

449

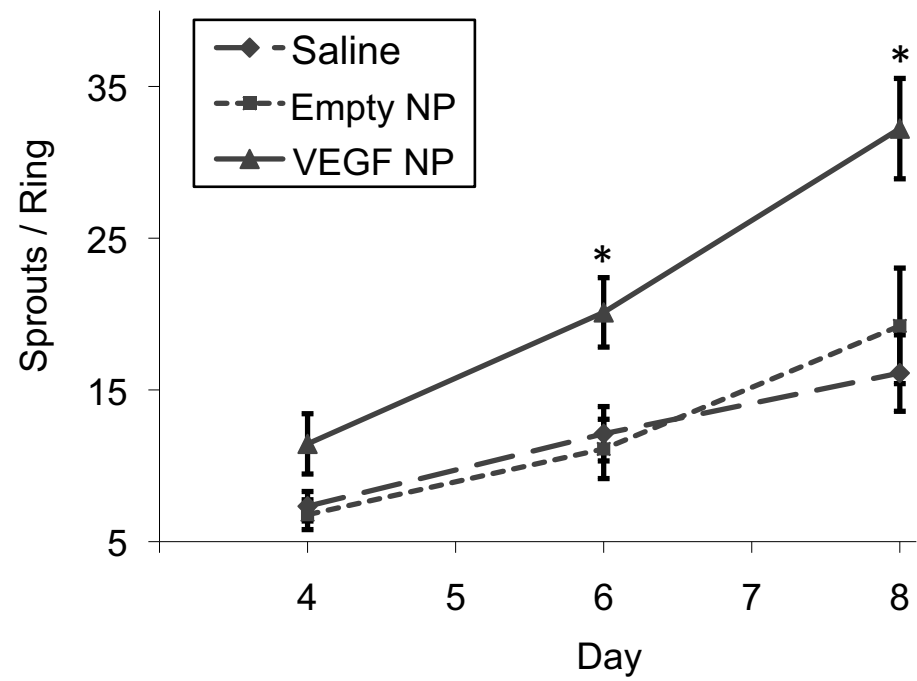
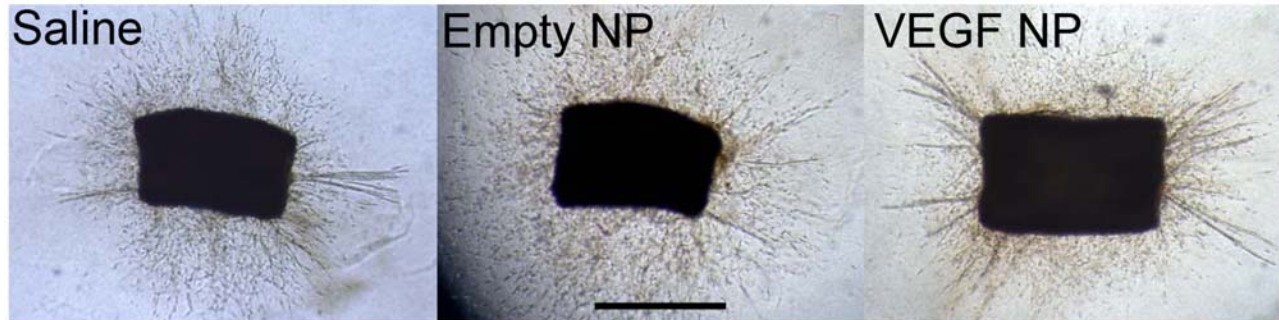
450 **Figure 5.** Vessel presence in ischemic hindlimb musculature (endothelial cells stained with
451 Lectin, nuclei were counterstained with Hoechst, 400X) (a) VEGF-NP (b) Saline (c) Non-
452 surgery/non-ischemic control limb.

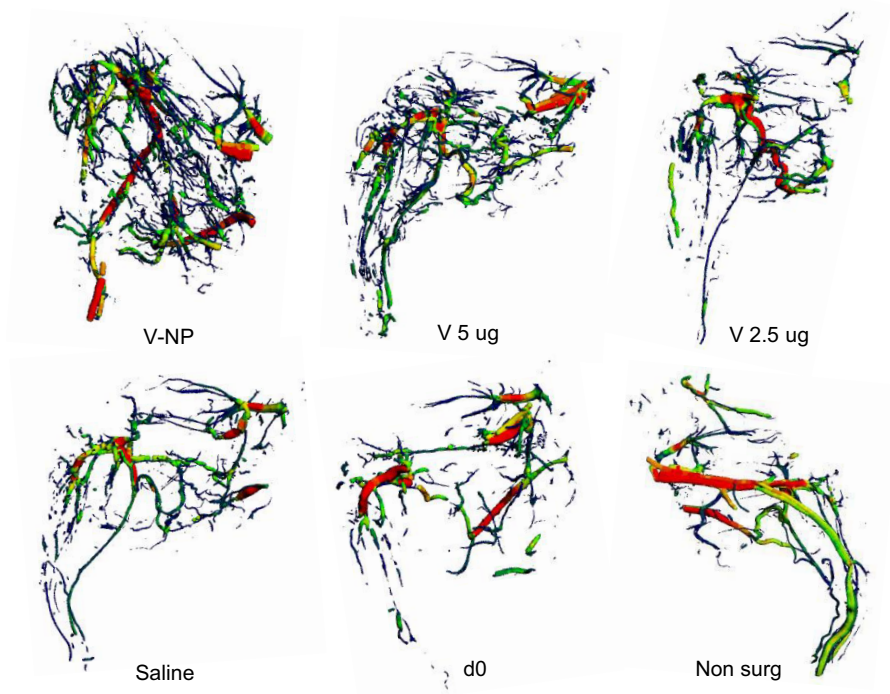


(a)

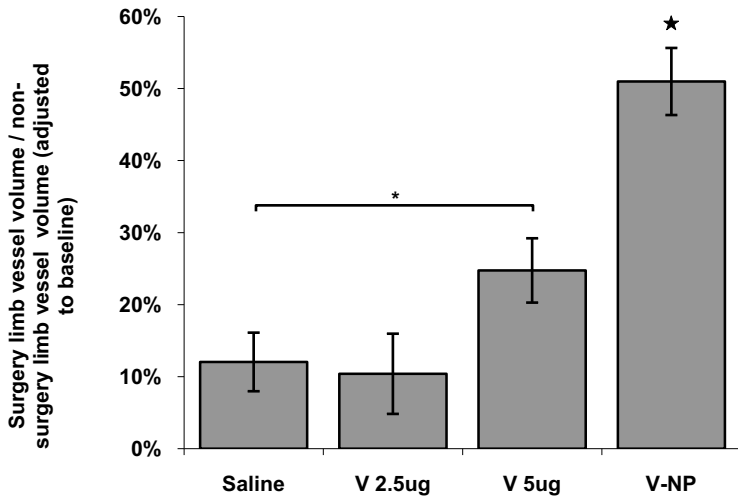


(b)

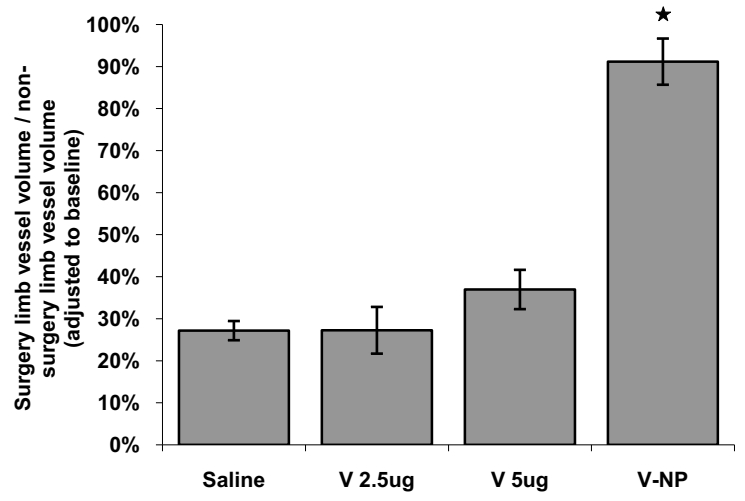




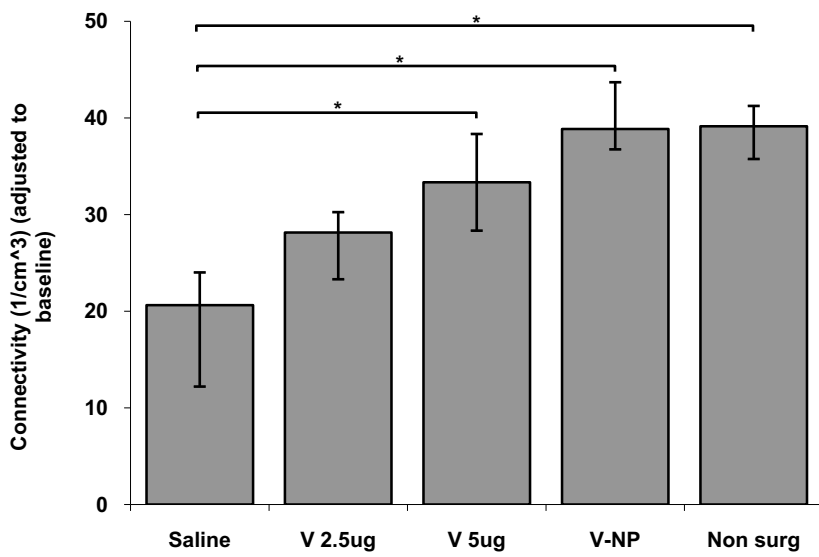
(a)



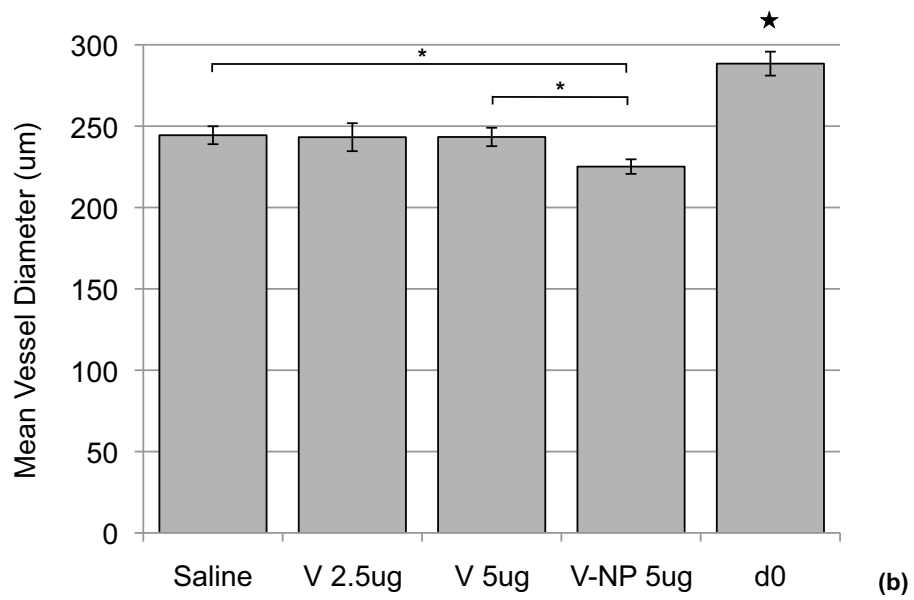
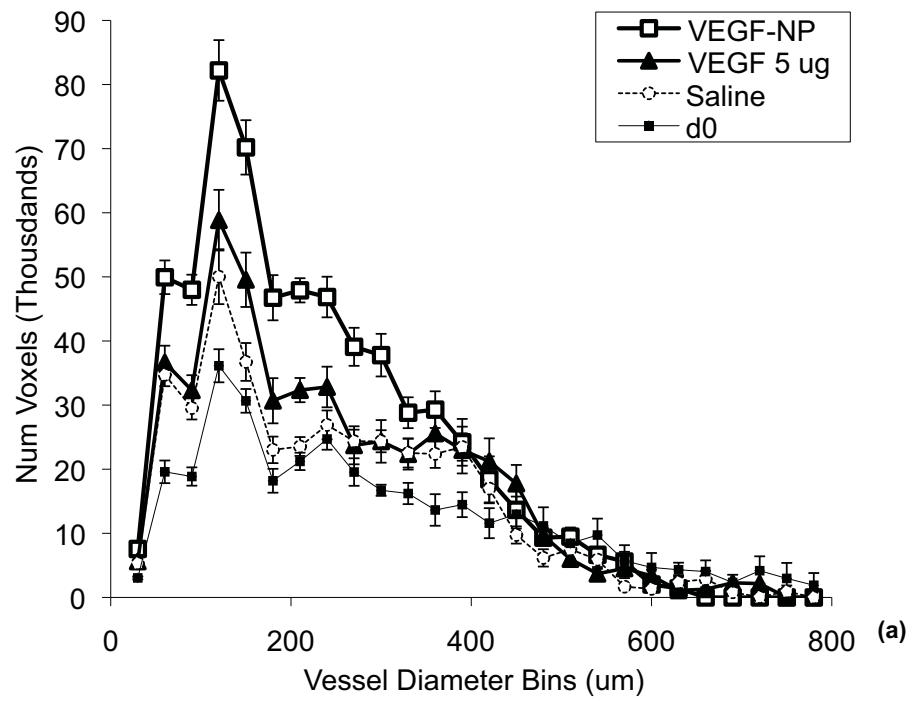
(b)

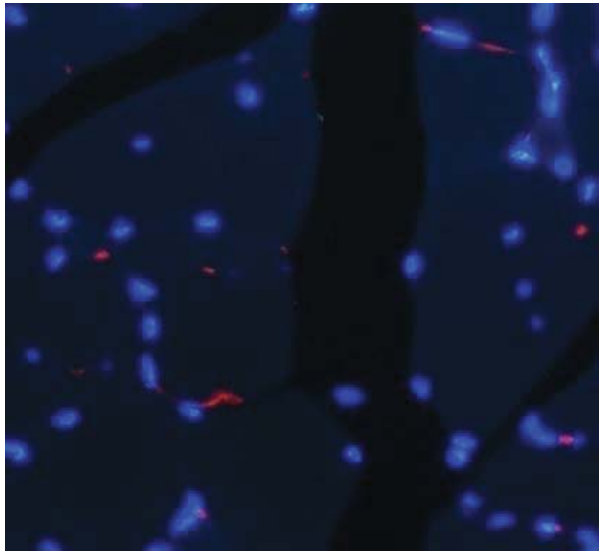


(c)

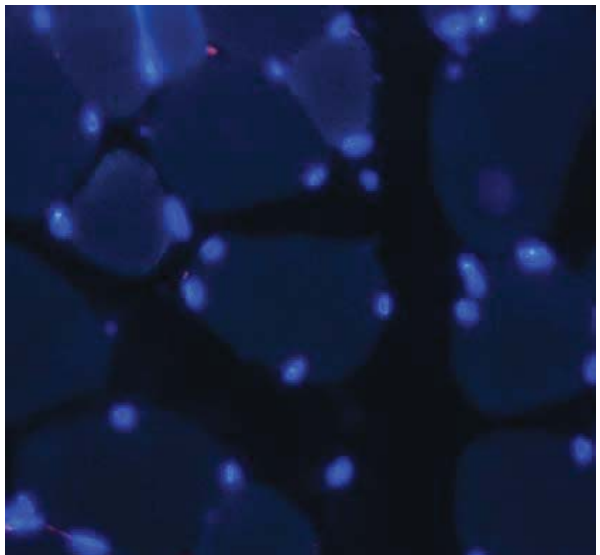


(d)

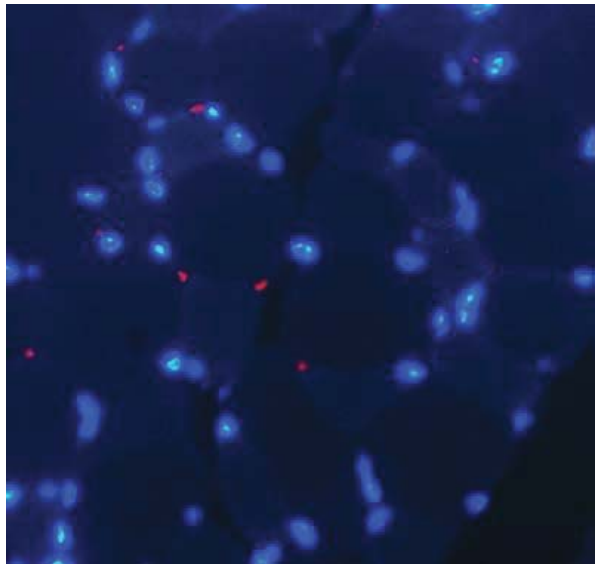




(a)



(b)



(c)